Magnetic anisotropy engineering in thin film Ni nanostructures by magneto-elastic coupling

S. Finizio,[1] M. Foerster,[1,2] M. Buzzi,[3] B. Krüger,[1] M. Jourdan,[1]
C.A.F. Vaz,[1,4] J. Hockel,[5] T. Miyawaki,[6] A. Tkach,[1] S. Valencia,[7]
F. Kronast,[7] G.P. Carman,[5] F. Nolting,[3] and M. Kläui[1,*]

[1]*Institut für Physik, Johannes Gutenberg Universität, Staudingerweg 7, Mainz, D-55128, Germany*

[2]*ALBA Synchrotron Light Source, Carretera BP 1413, km. 3.3 Cerdanyola del Valles, E-08290, Spain*

[3]*Swiss Light Source, Paul Scherrer Institut, Villigen, CH-5232, Switzerland*

[4]*SwissFEL, Paul Scherrer Institut, Villigen, CH-5232, Switzerland*

[5]*Department of Mechanical and Aerospace Engineering, University of California, Los Angeles, 90095, USA*

[6]*Department of Crystalline Materials Science, Nagoya University, Nagoya, 464-8603, Japan*

[7]*Helmholtz-Zentrum-Berlin für Materialien und Energie GmbH, Albert-Einstein Straße 15, Berlin, D-12489, Germany*

(Dated: November 27, 2013)

Abstract

We report a quantitative analysis of the magnetic uniaxial-anisotropy induced by piezoelectric strain in Ni nanostructured squares. By applying a strain, the magnetic domains in Ni nanostructured squares can be manipulated by the magneto-elastic effect in the Ni. The strain-induced anisotropy displaces the domain walls in the square (Landau state), leading to changes in the domain sizes. By comparing the experiments with micromagnetic simulations, the resulting uniaxial-anisotropy was quantified. A good agreement for a magnetostrictive constant of $\lambda_s = -26$ ppm was found, **confirming a full strain transfer from the piezoelectric to the Ni nanostructures and the retainment of a bulk-like magnetostrictive constant**.

Devices for spintronics applications are based on the manipulation of magnetization. Conspicuous examples include the control of the magnetization direction of ferromagnetic electrodes (e.g. in a magnetic tunneling junctions for MRAM applications [1]) or of ferromagnetic domains in nanowires (for storage class memory, such as the racetrack memory [2]). Conventionally, this manipulation is achieved by a current flowing through a coil or stripline, which generates an Oersted field. Another approach that has recently become very popular is to exploit the spin-torque effect due to a transfer of angular momentum from a spin polarized charge current [3]. However, such currents are always associated with unwanted heat dissipation in the device. An encouraging approach to achieve low power dissipation is based on the manipulation of magnetic ordering by the application of electrical fields. Different mechanisms where the application of an electric field leads to a change of magnetic properties have been suggested and studied. One promising approach is to use piezoelectric substrates or thin films onto which ferromagnetic layers of specific materials, such as Ni, are deposited. The piezo-active material generates a strain upon application of an electric field, inducing a strain in the magnetic film, which modifies the thin film crystal structure and, by spin-orbit coupling, this changes the magnetic properties of the ferromagnetic material. This effect, known as magneto-elastic coupling, allows one to induce phase-transitions, changes of the saturation magnetization, of the Curie temperature, and, most importantly, to manipulate the magnetic anisotropy [4–6]. The manipulation of the direction and strength of the uniaxial anisotropy is also ideal to achieve the switching of the magnetization direction, or to move domain walls. As thin film nanostructures are required for device applications, special attention needs to be paid **for** achieving the control of the magnetization in such nanoscale elements by magneto-elastic coupling.

Different piezoelectric materials can be used as substrates for ferromagnetic thin films. Key properties include the possible magnitude of static and dynamic strain, the compatibility with the growth of the magnetic thin films and the possibility to induce strain in a desired direction. One example is $[Pb(Mg_{0.33}Nb_{0.66})O_3]_{0.68}$-$[PbTiO_3]_{0.32}$ (PNM-PT), which exhibits a pseudocubic perovskite crystal structure with a lattice parameter of 4.02 Å [7] and which can be used to induce large strains in different directions depending on the crystalline orientation and resulting surface of the substrate [7, 8]. Such substrate material was previously successfully utilized, for instance, by Herklotz et al. [9] for the generation of strain in manganite thin films. While manganites are interesting for their complex magnetic and

electric properties, the relatively low Curie temperature (in particular of the surface magnetization [10]) makes the use of this compound in applications challenging. More suitable materials for applications are 3d metals, which exhibit reliable magnetic properties at room temperature. Moreover, if polycrystalline films can be utilized (as in the case of 3d metals), this makes the materials compatible with widespread applications, **but it is unclear if polycrystalline films exhibit the same large magnetostriction as the material in bulk form**. A suitable material, which has been used as bulk in the past to study magneto-elastic coupling, is Ni [5, 11]. In fact, thin films of Ni have recently been investigated and first studies of Ni nanostructures show a clear influence of the strain on the magnetization configuration [5, 12]. **As both the strain relaxation in thin layers and the polycrystalline nature of the Ni can reduce the magnitude of the magneto-elastic effect, rendering this applications-relevant system unsuitable, a careful quantification of the** effectively achievable magnitude of the magneto-elastic coupling still needs to be **carried out**. This is a crucial step towards potential applications, as it is not clear how large the achievable magnetic anisotropy changes are, since strain relaxation in buffer layers at edges and at grain boundaries, **combined with a reduced magnetostrictive constant for polycrystalline materials,** can limit the achievable magnetization changes.

In the work presented here, the strength of the magneto-elastic coupling in Ni nanostructures was determined by direct magnetic imaging in applied strain conditions. It was shown that the magnetization can be strongly modified by the induced strain even for moderate applied electric fields. By comparison with micromagnetic simulations, the induced anisotropy changes were evaluated, and it was found that, even for polycrystalline Ni on thick buffer layers, the magneto-elastic coupling is comparable to that found in bulk Ni, **showing negligible strain relaxation and no significant reduction in the magnetostrictive constant due to the polycrystalline nature of the Ni**.

The investigations presented in this article were carried out on 2 μm wide Ni squares. The samples were fabricated by depositing 35 nm of Ni by electron beam evaporation on top of a 50 nm sputter-deposited buffer Pt electrode (with a 5 nm Ti adhesion layer), grown on a 0.5 mm thick PMN-PT (011) substrate (Atom Optics Co., Ltd., Shanghai, China) in the as-received condition (i.e. no electrical poling prior to the deposition of the Ni). Patterning was carried out by electron-beam lithography employing a lift-off technique. Further details on the deposition procedure and on the fabrication of the nanostructures can be found in [5].

The average size of the polycrystalline grains, determined by XRD analyses on continuous films grown in the conditions used here is about 10 nm. A schematic of the analyzed samples is shown in Fig. 1(a), where also a scanning electron microscopy (SEM) image of a 2 μm-wide square structures is presented (Fig. 1(b)).

Imaging of the magnetic configuration of the nanostructures was carried out by photoemission electron microscopy (PEEM) utilizing the X-ray magnetic circular dichroism effect (XMCD) to obtain magnetic contrast [13]. The sample was illuminated by circularly polarized X-rays tuned to the L_3 edge of Ni (852.5 eV). All measurements were carried out at room temperatures at the beamline UE-49-PGM-a at BESSY II, Berlin [14] and at the beamline SIM (X11MA) at SLS, Villigen [15], both equipped with an Elmitec PEEM setup (type LEEM III). Electric fields were applied to the piezoelectric material by a floating voltage generator inside the high voltage environment of the PEEM control unit; contacting was carried out as shown in Fig. 1(a). **The sample was attached to the PEEM sample holder in a single location, with the a silver colloidal solution. This particular arrangement allows for the free expansion of the substrate in all spatial directions, to prevent any clamping and use the full strain generated by the piezoelectric substrate.**

For the analyses presented here, a particularly apt geometry is the high symmetry square as, for a broad range of lateral sizes and film thicknesses, this geometry allows for the formation of the simple magnetic flux-closure Landau state [16], where four equally sized domains are formed due to shape anisotropy, as shown in Fig. 2. As the anisotropy is changed, the size of the magnetic domains changes and domains with the magnetization pointing along an easy axis grow, while perpendicular domains with magnetization along the hard axis shrink. Thus, the size of the domains, which can be experimentally measured by magnetic microscopy, acts as an indicator of the magnitude of the anisotropies applied to the magnetic material.

The PMN-PT was oriented in the (011) direction, which enables the generation of an in-plane strain by applying an out of plane electric field [7, 8]. The piezoelectric strain behaves hysteretically with respect to the applied electric field, as shown in Fig. 1(c). However, after an initial poling of the piezoelectric material (the substrate was initialized with a field of 0.6 MV m^{-1}), it is possible to achieve a linear non-hysteretic behavior by restricting the applied electric field to a range in which the polarization of the substrate is not reversed. Fields

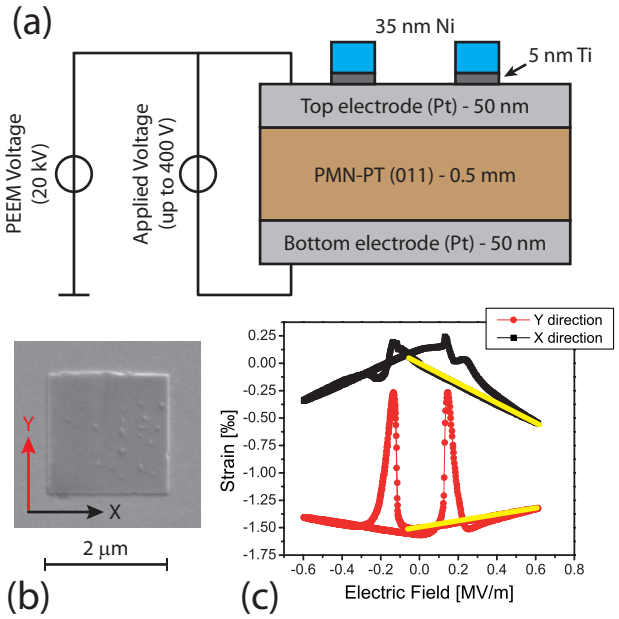

Figure 1. (color online) (a) Schematic of the sample structure, including the electrical contact setup; (b) Scanning electron micrograph of a 2 μm-wide Ni square structure. Indicated are the x and y directions shown in (c); (c) Hysteresis cycle of the in-plane strain (x and y directions) as a function of the applied out of plane electric field (z direction) of a PMN-PT (011) substrate. Adapted from [8]. The yellow line indicates the electric field range used in the experiments described here.

between -0.1 and 0.6 MV m^{-1} (as marked in Fig. 1(c), where a positive field corresponds to a positive voltage applied to the bottom electrode with respect to the top electrode) were applied during the experiments presented here. **A concern is the influence of the 50-nm thick Pt buffer layer, which can reduce the strain transfer from the substrate to the Ni nanostructures. While any shear lag effect in the nanostructures can be expected to extend laterally only for a distance corresponding to ca. 2-3 times the thickness into the nanostructure, strain relaxation in the material can play a role, as frequently observed in epitaxial growth, for which strain relaxation can set in after a few monolayers.**

For the geometry used here, the magnetic ground state is the Landau state. However, due to the finite probability of electrical discharges naturally inherent to the PEEM setup, which lead to strong magnetic fields on the sample, it is also possible to nucleate more complex metastable states due to electric discharges in the PEEM. In this case, the Landau state [16] is recovered by demagnetizing the system by applying alternating magnetic fields with an in-situ electromagnet.

To study the induced magnetic anisotropies, the magnetic configuration of the Ni square

was imaged as a function of the electric field applied to the substrate, i.e. for different strain conditions, as shown in Fig. 2(a). The central image in Fig. 2(a) is showing a symmetric Landau state, which corresponds to the unstrained, shape-anisotropy dominated state. With the application of strain, two domains (with antiparallel magnetization) grow in size, while the other two with magnetization perpendicular to the other two domains shrink. Domains with magnetization parallel to the applied compressive strain (indicated by the blue arrows) grow in size at the expense of the domains with perpendicular magnetization (parallel to the tensile strain indicated by the yellow arrows). This is a direct evidence that an uniaxial anisotropy is induced in the magnetic material upon the application of piezoelectric strain. The observed behavior is qualitatively in line with the expected behavior of Ni, which, given the negative sign of its magnetostrictive constant (in bulk Ni, $\lambda_s \simeq$ -32 ppm [17]), should indeed present a growth of the magnetic domains pointing along the direction of the compressive strain.

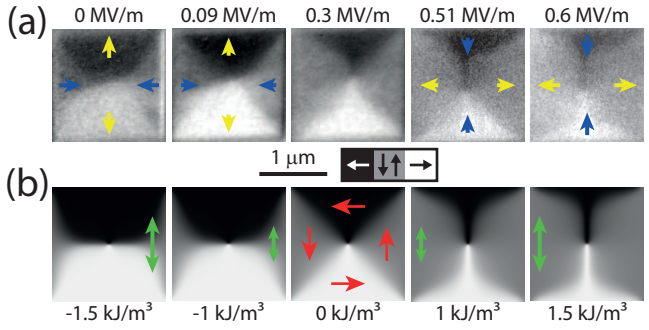

Figure 2. (a) XMCD-PEEM images of a 2 μm wide Ni square, at different applied electric fields. The blue and yellow arrows indicate the directions of the compressive and tensile strain, respectively. (b) Micromagnetic simulations of a 2 μm wide Ni square, assuming different uniaxial anisotropies. The grayscale bar and the red arrows indicate the direction of the magnetic contrast, while the green arrow indicates the direction of the uniaxial anisotropy applied in the micromagnetic simulations.

Next, the induced anisotropies were quantified. To conduct this analysis, the size of the domains with magnetization parallel or perpendicular to the applied compressive strain direction was determined as function of the applied electric field (i.e. piezoelectric strain), as shown in Fig. 3. Corresponding micromagnetic simulations of a 2 μm wide Ni square with different anisotropies were then carried out, to find for which anisotropy values the domain configurations agree.

The simulations were carried out utilizing the MicroMagnum framework [18], with the following parameters for Ni: exchange constant 10^{-11} J m^{-1} and saturation magnetization

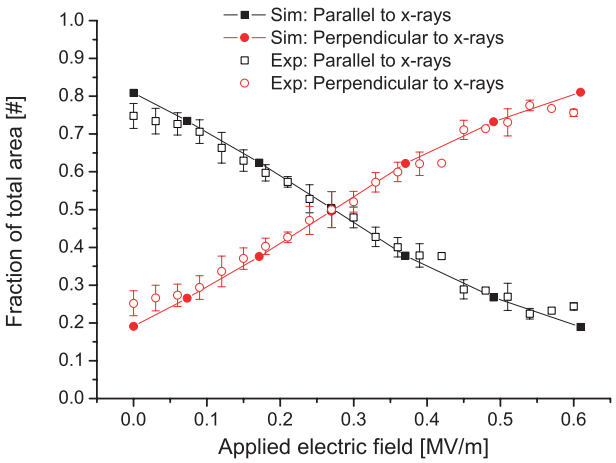

Figure 3. Fraction of the area occupied by domains with magnetization parallel (black square symbols) and perpendicular (red circle symbols) to the x-ray beam (i.e. size of black/white and grey areas in the images). The empty squares and circles indicate data points determined from the experimentally obtained images, the full squares and circles indicate data points determined from the simulated images. The lines are guides to the eye.

$2.1 \cdot 10^5$ A m^{-1}, determined by SQUID analysis on a continuous Ni film of similar characteristics. These parameters lead to an exchange length of $\simeq 18$ nm. The numerical discretization utilized for the calculations presents a cell size of 8 nm in the in-plane direction and 35 nm in the out-of-plane direction (the total thickness of the structure is 35 nm). **The fact that the determined agreement is similarly good everywhere in the nanostructure allows one to observe that shear lag effects at the edges of the nanostructure are not significantly altering the magnetic propeties.**

The simulations were carried out for a range of anisotropies, as shown in Fig. 2(b), to simulate the contribution of the applied piezoelectric strain, checking the validity of the simulations by comparing the simulated configurations and XMCD-PEEM images of the Ni square as function of an externally applied magnetic field, which yield good agreement. In order to directly compare the experimental images with the micromagnetic simulations, the simulated uniaxial anisotropy has been converted to an effective applied strain by using the following relation [19]:

$$\mathrm{K_{ME}} = -\frac{3}{2}\lambda_\mathrm{s}\mathrm{Y}\left|\varepsilon_x - \varepsilon_y\right|, \tag{1}$$

where $\mathrm{K_{ME}}$ denotes the magneto-elastic anisotropy coefficient, λ_s the magnetostrictive constant of Ni, Y the Young's modulus of Ni, and $|\varepsilon_x - \varepsilon_y|$ the in-plane strain difference. A value of 220 GPa has been utilized for the Young's modulus, which corresponds to the value

measured in bulk Ni [20]. The adoption of the bulk value for the Young's modulus constitutes an approximation for the analyzed material. However, as the size of the grains is small (ca. 10 nm) compared to the size of the structures, the usage of the bulk value for the Young's modulus constitutes a reasonable approximation. The value of $|\varepsilon_x - \varepsilon_y|$ was then converted to an effective applied electric field by using the strain-vs-field curve of PMN-PT (011).

Due to the polycrystalline nature of the Ni (i.e. no effective magneto-crystalline anisotropy is present due to the random orientation of the many grains), the micromagnetic simulations do not include any additional anisotropy contribution besides the one arising from the applied strain. Note that the zero strain condition at which the magnetic state of the Ni square falls into a symmetric Landau state was achieved with an applied electric field of $\simeq 0.27$ MV m^{-1}. Since there is no further externally applied electric fields to induce a strain, this implies that a pre-existing anisotropy is present. This may be related to the thin film deposition on the PNM-PT substrate without prior poling, i.e. on a substrate with different ferroelectric domains resulting in regions with different pre-strain after poling [12]. Another possible origin of the pre-existing anisotropy can be due to microscopic step formation on the substrate surface due to a miscut.

Thus, the zero in $|\varepsilon_x - \varepsilon_y|$ of eq. (1) was shifted to the value of the strain condition at which the un-perturbed Landau state was observed experimentally. Such an un-perturbed Landau state results from zero strain and zero anisotropy (with the exception of shape anisotropy), and thus allows for the identification of the strain-free condition. With this adjustment, the experimental data fits well with the simulations with a magnetostrictive constant $\lambda_s = -26$ ppm, which is within the range typically found for bulk Ni.

In the electric field range analyzed, the fraction of the total area occupied by the magnetic domains pointing along the compressive strain direction scales almost linearly with the applied field. For larger field values, deviations from the linear behaviour are observed, due to the increasing shape anisotropy contribution, which counteracts the induced anisotropy. The simulations show that, for high strains (not achievable experimentally due to dielectric breakdown of the substrate), the dimensions of the domain walls pointing along the compressive strain direction saturate, due to the dominant role of the shape anisotropy.

The value of the magnetostrictive constant which was found from the simulations is about 10% smaller than the bulk value. This might be due to strain relaxation in the buffer layer

and to the polycrystalline nature of the deposited material, but shows that a very sizeable magneto-elastic coupling can be obtained.

In conclusion, we have achieved a manipulation of the magnetic configuration of Ni nanostructured squares **without any electrical currents** by applying **only** electrical fields to a piezo-substrate. The manipulation of the magnetic configuration is achieved by the exploitation of the magneto-elastic effect, which originates from the strain induced by the piezoelectric substrate of the nanostructures. We find that the domain walls of a magnetic square in the Landau state can be reversibly displaced by the induced anisotropy leading to a change in the domain size. Combining the experimental results with micromagnetic simulations, we determine the resulting uniaxial anisotropy quantitatively. We find a good quantitative agreement for a magnetostrictive constant of the Ni nanostructures of $\lambda_s = -26$ ppm, which is only slightly smaller than the bulk value of Ni. **The calculated value of the magnetostrictive constant can only be explained if the strain transfer from the substrate to the nanostructures across the buffer layer happens with negligible relaxation effects, and if the polycrystalline Ni shows a magnetostrictive constant comparable to that of the single crystalline Ni.** This shows that even for thick buffer layers and polycrystalline films large effects can be obtained for these applications' relevant nanostructures.

Part of this work was performed at the Swiss Light Source, Paul Scherrer Institut, Villigen, Switzerland and at the Helmholtz-Zentrum-Berlin, Germany. The authors further acknowledge the financial support by the EU's 7th Framework Programme IFOX (NMP3-LA-2010 246102), the European Research Council through the Starting Independent Researcher Grant MASPIC (ERC-2007-StG 208162), the National Science Foundation under award number 1160504 NSF Nanosystems Engineering Research Center for Translational Applications of Nanoscale Multiferroic Systems (TANMS), the Swiss National Science Foundation, the Graduate School of Excellence "Materials Science in Mainz" (GSC 266), and the Deutsche Forschungsgemeinschaft (DFG).

* Corresponding Author: klaeui@uni-mainz.de

[1] J. Åckereman, Science **308**, 508 (2005).

[2] S. Parkin, M. Hayashi, and L. Thomas, Science **320**, 5873 (2008).

[3] J. Katine, F. Albert, R. Buhrman, E. Myers, and D. Ralph, Physical Review Letters **84**, 3149 (2000).

[4] M. Liu, J. Hoffman, J. Wang, J. Zhang, and B. Nelson-Cheeseman, Scientific Reports **3**, 1876 (2013).

[5] J. Hockel, A. Bur, T. Wu, K. Wetzlar, and G. Carman, Applied Physics Letters **100**, 022401 (2012).

[6] C. Adamo, X. Ke, H. Wang, H. Xin, T. Heeg, M. Hawley, W. Zander, J. Schubert, P. Schiffer, D. Muller, L. Maritato, and D. Schlom, Applied Physics Letters **95**, 112504 (2009).

[7] K. Uchino, Ferroelectrics **151**, 321 (1994).

[8] T. Wu, P. Zhao, M. Bao, A. Bur, J. Hockel, K. Wond, K. Mohachandra, C. Lynch, and G. Carman, Journal of Applied Physics **109**, 124101 (2011).

[9] A. Herklotz, J. Plumhof, A. Rastelli, O. Schmidt, L. Schultz, and K. Dörr, Journal of Applied Physics **108**, 094101 (2010).

[10] R. Reeve, C. Mix, M. König, M. Foerster, G. Jakob, and M. Kläui, Applied Physics Letters **102**, 122407 (2013).

[11] A. Bur, T. Wu, J. Hockel, C.-J. Hsu, H. Kim, T.-K. Chung, K. Wong, K. Wang, and G. Carman, Journal of Applied Physics **109**, 123903 (2011).

[12] M. Buzzi, R. Chopdekar, J. Hockel, A. Bur, T. Wu, N. Pilet, G. Carman, L. Heyderman, and F. Nolting, Physical Review Letters **111**, 027204 (2013).

[13] J. Stöhr, Y. Wu, B. Hermsmeier, M. Samant, G. Harp, S. Koranda, D. Dunham, and B. Tonner, Science **259**, 658 (1993).

[14] F. Kronast, J. Schlichting, F. Radu, S. Mishra, T. Noll, and H. Durr, Surface and Interface Analysis **42**, 1532 (2010).

[15] U. Flechsig, F. Nolting, A. Fraile-Rodriguez, J. Krempasky, C. Quitmann, T. Schmidt, S. Spielmann, and D. Zimoch, AIP Conference Proceedings **1234**, 319 (2010).

[16] A. Hubert and R. Schäfer, *Magnetic Domains: The Analysis of Magnetic Microstructures* (Springer-Verlag, Berlin, 1998).

[17] R. Cullity and C. Graham, *Introduction to Magnetic Materials* (Wiley-IEEE Press, 2008).

[18] C. Abert, G. Selke, B. Krüger, and A. Drews, IEEE Transactions on Magnetics **48**, 1105 (2012).

[19] M. Weiler, A. Brandlmaier, S. Geprägs, M. Althammer, M. Opel, C. Bihler, H. Huebl, M. Brandt, R. Gross, and S. Goennenwein, New Journal of Physics **11**, 013021 (2009).

[20] H. Ledbetter and R. Reed, Journal of Physical and Chemical Reference Data **2**, 531 (1973).